Femtosecond relaxation dynamics of image-potential states

R. W. Schoenlein* and J. G. Fujimoto
Department of Electrical Engineering and Computer Science and Research Laboratory of Electronics, Massachusetts Institute of Technology, Cambridge, Massachusetts 02139

G. L. Eesley and T. W. Capehart
Department of Physics, General Motors Research Laboratories, Warren, Michigan 48090
(Received 18 June 1990)

Relaxation dynamics of the $n=1$ and 2 image-potential states on Ag(100) and Ag(111) are investigated using femtosecond pump-probe techniques. Transient two-photon photoemission measurements are performed using femtosecond pulses with photon energies of 2.00 and 4.00 to 4.35 eV, generated via self-phase modulation and frequency doubling. We measure the lifetime of the $n=1$ and 2 image states on Ag(100) to be 25 ± 10 and 180 ± 20 fs, respectively. The lifetimes are within the range predicted by theoretical models, and are consistent with the expected n^3 lifetime scaling. In contrast, measurements of the $n=1$ and 2 image states on Ag(111) reveal substantially shorter lifetimes, <20 fs. This compares favorably with recent theoretical models that predict shorter lifetimes due to the structure of the (111) surface and its effect on the image-potential states.

I. INTRODUCTION

Image-potential states are an interesting class of surface states occurring at the interface between the crystal lattice and the vacuum. Image states are formed by the Coulombic attraction between an electron existing outside a crystal surface and its image charge in the solid. The electron is trapped by the Coulomb potential in the vacuum, and by a gap of available bulk states. This two-dimensional electron confinement is analogous to quantum well states in semiconductors. However, since these states are localized in the vacuum, they are relatively unaffected by bulk scattering processes and are expected to be long lived relative to bulk states in metals at comparable excess energies. They provide a unique opportunity for studying the dynamics of a two-dimensional electron gas in vacuum.

Shockley first suggested the existence of image-potential states over 50 years ago,[1] though he did not specify the conditions necessary for their existence. Early theoretical treatments of image-potential states established the validity of a simple hydrogenic model, consisting of a Coulomb potential modified by the static dielectric constant of the material.[2] This model accurately predicts a Rydberg-like series of bound states approaching the vacuum level, with binding energies $E_n \sim 1/n^2$. In the past several years, the simple hydrogenic model of image-potential states has been refined. Recently, many-body calculations of the wave-function self-energy have been used to predict image-state lifetimes, and lifetime scaling with state number n for various metal surfaces.

The first experimental evidence of image-potential states on metal surfaces was obtained only a few years ago by Johnson and Smith using inverse photoemission techniques.[3,4] More recently, binding energies for the $n=1$ and 2 states on surfaces of single-crystal Ag, Cu, and Ni have been determined by Giesen *et al.* using high-resolution two-photon photoemission.[5-8] Binding energies of image states on various surfaces have also been measured using angle-resolved inverse photoemission.[9-16]

However, previous experimental studies of image-potential states have been unable to provide conclusive information about the lifetimes of these states. Since image states are relatively insensitive to phonon scattering and other energy-loss mechanisms associated with the crystal, they are expected to be long lived relative to bulk states. As expected, the observed linewidth broadening is quite small, <100 meV,[5-7] but measurement accuracy has been limited by instrument resolution and work function inhomogeneities.

Experimental results presented in this paper represent the first direct measurement of image-potential state lifetimes. These measurements are an important test of the theoretical models because they show how image-state lifetimes scale with the state number. In addition, measurements from different surfaces give some indication of how excited-state lifetimes can be affected by the position of the image states within the bulk band gap. We present experimental studies of the femtosecond transient dynamics of the $n=1$ and 2 image-potential states on the (100) and (111) surfaces of Ag.[17,18] Ultraviolet pump and visible probe techniques are combined with two-photon photoemission spectroscopy to investigate the excitation and relaxation processes in time and energy.

II. EXPERIMENT

A. Image states on Ag(100)

Studies of image-state relaxation dynamics are performed with a femtosecond laser system consisting of a

dispersion-compensated colliding-pulse mode-locked ring dye laser[19] and a copper vapor laser amplifier.[20] The system operates at 8 kHz, and produces 50-fs pulses at 620 nm (2.00 eV) with energies of more than 2 μJ per pulse. Amplified pulses are split into pump and probe in a 70:30 (pump:probe) power ratio by a beamsplitter. The probe is delayed with respect to the pump by a computer-controlled translation stage with 0.1 μm step size.

Ultraviolet pulses at 4.00 eV photon energy are generated in the pump arm by frequency doubling the fundamental femtosecond pulses in a crystal of potassium dihydrogen phosphate (KDP). We use a crystal which is only 100 μm thick in order to minimize pulse-broadening effects due to phase-matching limitations between the visible and ultraviolet pulses.

The ultraviolet pulses are also broadened after the generation process by group velocity dispersion due to the optical elements (lenses and windows). These effects are minimized by using low dispersion materials, and short interaction lengths. Second-order dispersion of the uv pulses is compensated using a pair of quartz prisms which are arranged to provide negative group velocity dispersion.[21] Using this approach, we are able to generate uv pulses as short as 50 fs at 4.00 eV. The uv and visible pulses are combined in a collinear geometry using a dichroic mirror, and enter an ultrahigh-vacuum chamber (base pressure $\sim 10^{-10}$ Torr) through a $\frac{1}{8}$-inch-thick fused silica window. A curved aluminum mirror (50 mm focal length) is used inside the chamber to focus the pulses to a spot size of ~ 20 μm on the sample surface.

The Ag(100) sample is cut and mechanically polished in a (100) orientation within $\pm 2°$. The sample is positioned in front of a double-pass cylindrical mirror analyzer (CMA) which is used to collect the photoelectrons. A potential bias of 5–10 V is applied between the sample and the CMA to minimize the effects of stray fields and facilitate electron collection. The CMA has an energy resolution of ~ 180 meV, and a nominal collection angle of $\sim 12°$. By appropriately positioning the sample, we are able to reduce the angular resolution to $< 10°$. After repeated cycles of sputter ion cleaning and annealing, the surface quality was verified using low-energy electron diffraction (LEED) and Auger spectroscopy.

Figure 1 shows an energy-level diagram of the Ag(100) surface, and a projection of the bulk band structure for $k_{\parallel}[100]=0$. Electrons are confined in the orthogonal direction, resulting in discrete states with binding energies of 0.53 ± 0.02 and 0.16 ± 0.02 eV for $n=1$ and 2, respectively.[7] In the $k_{\parallel}[100]$ direction, the bands are nearly free-electron-like with an effective mass of $1.15 m_0$ for $n=1$ electrons.[22] Since there are no occupied surface states below the Fermi energy for the (100) crystal orientation, the $n=1$ image-potential state is populated via nonresonant transitions from occupied bulk states. Because we use two different wavelengths, various excitation and photoemission processes are energetically allowed.

The $n=1$ state may be populated via electronic transitions with either one 4.0-eV photon, or two 2.0-eV photons. Since the $n=1$ state is 3.90 eV above the Fermi energy, these transitions result in a distribution of excited electrons which extends ~ 100 meV from the bottom of the $n=1$ band. Electrons are then emitted from the $n=1$ state by either 2.0 or 4.0-eV photons. These photon energies are not sufficient to populate the $n=2$ state because it lies 4.27 eV above the Fermi level.

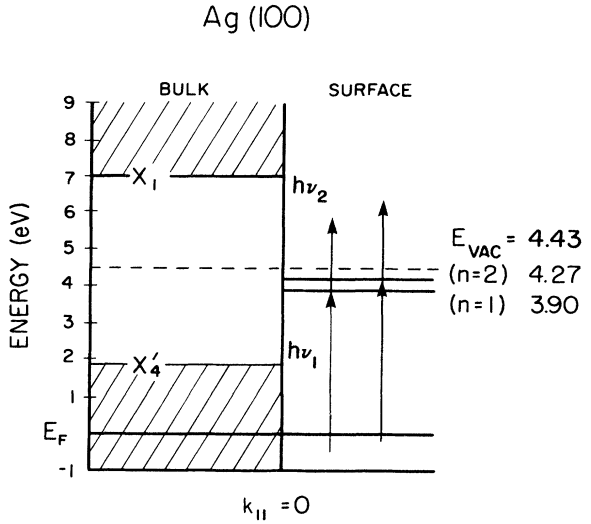

FIG. 1. Energy-level diagram of Ag(100) surface states, and bulk band projections for $k_{\parallel}[100]=0$. Ultraviolet femtosecond pulses, $h\nu_1=4.00$ eV (4.35 eV), populate the $n=1$ (and $n=2$) states via nonresonant transitions originating below the Fermi level. Visible pulses, $h\nu_2=2.00$ eV, photoemit electrons to the vacuum.

In addition to the transitions described above, other photoemission processes can occur which do not couple to the image-potential states. These are multiphoton processes, and may originate in the bulk or at the surface. The dominant non-image-state effect is photoemission involving two uv (4.0-eV) photons. In this process, one uv photon excites electrons from the d bands to empty states above the Fermi level. The second uv photon then photoemits these electrons to the vacuum, resulting in a photoelectron distribution which is concentrated at low energies, ~ 1 eV or less.

Furthermore, nonequilibrium electron heating[23] from the femtosecond pulses will smear the electron distribution about the Fermi energy. Electrons in the high-energy tail of the distribution may then be photoemitted to the vacuum, contributing to the photoelectron yield at low energies. In addition, photoemission involving three visible (2.0-eV) photons can occur. However, if the transitions do not couple to the $n=1$ image-potential state, then they must involve two virtual states, and the cross section for this process is very small.

The dynamics of the $n=1$ image-potential state may be studied using the two-photon uv process, or the three-photon visible process. However, both of these approaches result in time-resolved data which are symmetric with respect to time delay and therefore difficult to interpret. The uv-only process has the additional

disadvantage of relatively large background levels. The visible-only process is essentially background-free, but is further complicated by the fact that it is a third-order effect.

In our studies of the $n=1$ image-potential state dynamics, we populate the state with an uv (4.0-eV) pulse and then probe the transient response by photoemitting electrons to the vacuum with a delayed visible (2.0-eV) pulse. This two wavelength technique is important in time-resolved photoemission because it breaks the symmetry of standard two-photon photoemission, allowing independent control of polarization and a separation of pump effects from those of the probe. The added degree of freedom is instrumental in isolating specific electronic transitions in more complicated systems and permits nearly background-free measurements of electron energy spectra on a femtosecond time scale.

Furthermore, photoemission from image-potential states using a single 2.0-eV photon is more efficient than photoemission with an uv photon since most of the uv energy, $\sim 90\%$, is absorbed via d-band transitions. Thus measurements can be performed at the lowest possible uv fluences, thereby limiting the effects of nonequilibrium electron heating generated by femtosecond pulses and suppressing the two-photon background photoemission signal from the uv pulses. We do observe a background signal due to three- (2.0-eV) photon photoemission via the $n=1$ image state, however, the signal is substantially lower than the uv-visible two-photon signal since the process is third order.

In all uv-visible measurements the photoemission yield scales linearly with both uv and visible fluences. Verification of this scaling is important to ensure that space-charge screening effects are not present. Photoelectron energies are measured relative to the vacuum potential which is determined by the onset of the photoemission signal. We use p polarization in order to satisfy transition selection rules. Some photoemission is observed with s-polarized light, but the yield is diminished by a factor of 30. The residual signal is attributed to surface photoemission as well as bulk photoemission processes from depolarization of the beam caused by stress-induced birefringence in the fused silica vacuum window.

Figure 2 shows a series of two-photon (4.0 eV pump and 2.0 eV probe) photoemission spectra taken at various time delays with positive delay corresponding to visible femtosecond pulses arriving after the uv pulses. The uv and visible fluences are $\sim 6\times 10^{-2}$ and ~ 0.7 mJ/cm^2, respectively (assuming a 20-μm spot size), which generate maximum nonequilibrium electron temperatures of a few hundred degrees. This heating has a negligible effect on our image-potential state measurements since the uv pump transitions originate ~ 100 meV below the Fermi level. The peak photoelectron yield is ~ 600 counts per second (7.5×10^{-2} electrons/pulse), corresponding to a quantum efficiency on the order of 10^{-11} electrons per uv and visible photon.

The transient photoemission energy spectra show the dynamics of the image-potential state in both energy and time. The rising signal at early times indicates the population of the image state by the femtosecond uv pulse.

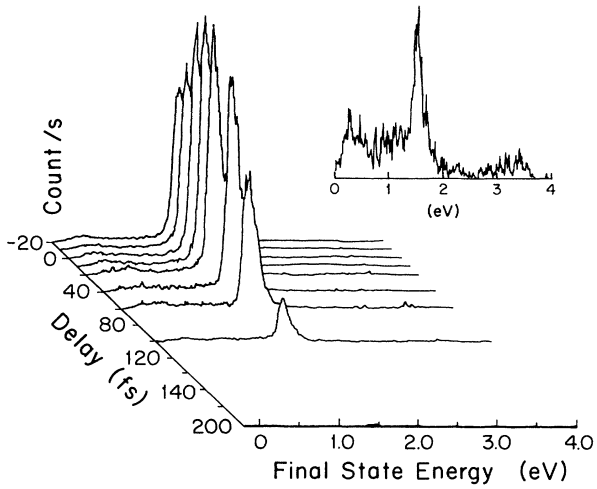

FIG. 2. Photoelectron spectra at various time delays showing the dynamics of the $n=1$ state on Ag(100). Inset (100× vertical scale): the background spectra at +200 fs delay.

Spectra at later times show the decay of the excited state within the first 100 fs. The peak appears at ~ 1.5 eV which corresponds to the $n=1$ image-potential state lying ~ 0.5 eV below the vacuum level and is consistent with previously reported results.[7] As expected, the position of this peak remains invariant over the lifetime of the state. Photoemission from the $n=2$ state is not observed since the 4.0 eV pump photon energy is not sufficient to populate this level.

We measure an energy width of less than 200 meV, which is close to the resolution of our CMA. In general, there are two contributions to this measured width. One is linewidth broadening due to the finite lifetime of the excited state. A second contribution comes from dispersion of the $n=1$ band in the $k_{\parallel}[100]$ direction ($m_{\text{eff}}=1.15m_0$). Because of the CMA angular resolution, our measurements are sensitive to electrons with nonzero transverse momentum, $k_{\parallel}[100]$. However, this contribution to the measured energy width is only ~ 40 meV. Thus the observed linewidth is primarily determined by the energy resolution of the CMA.

The background photoelectron spectra (inset, 100× vertical scale) measured at +200 fs delay, is shown for reference. We observe a peak at 1.5 eV resulting from three- (2.0-eV) photon photoemission via the $n=1$ image-potential state and a peak at 3.5 eV corresponding to two- (4.0-eV) photon photoemission from the $n=1$ state. At these time delays we do not detect any photoemission from the combination of uv and visible pulses.

Deconvolution of the transient photoelectron spectra (assuming an energy resolution of 180 meV) indicates an $n=1$ lifetime on the order of the pulse duration. Quantitative results are obtained through time-resolved measurements of the photoemission yield at the peak of the energy distribution. However, accurate analysis depends on the determination of the zero delay as well as the uv-visible cross-correlation width. The lifetime of the image-potential state can be quenched by adsorbing im-

purities on the (100) surface, thereby providing additional relaxation channels. Under these conditions, the transient response of the $n=1$ state gives an accurate estimate of the pulse cross correlation as well as the zero delay at the sample surface.

Figure 3 shows the dynamics of the $n=1$ state for electrons near the bottom of the image-potential band (energy analyzer tuned to 1.5 eV). The solid line is a measure of the image-state lifetime on a clean Ag(100) surface, and the dotted line is a measure of the photoemission from an oxygen-dosed ($\sim 3\times 10^{-4}$ Torr s) surface taken under identical experimental conditions.

The photoemission measurement from the clean surface displays a distinct asymmetry and the peak is shifted toward positive delay (visible following uv) relative to the measurement of the oxygen-dosed surface. This clearly demonstrates the finite duration of the measured lifetime. The asymmetry corresponds to population of the state with uv pulses and photoemission with delayed visible pulses. Because of the finite lifetime, electrons accumulate in the $n=1$ state after the peak of the uv pulse, thus the maximum photoemission yield occurs after the zero delay.

The measurement from the oxygen-dosed surface is quite symmetric, and the peak signal level is substantially lower, suggesting that the image-state lifetime under these conditions is nearly instantaneous. Measurements of the photoelectron energy distribution show a peak width of ~ 270 meV for the $n=1$ state on the oxygen-dosed surface. Considering the ~ 180-meV resolution of the CMA, this suggests that the oxygen-dosed lifetime is only a few femtoseconds. Auger electron spectroscopy (AES) indicates that the surface is not saturated with oxygen. However, inhomogeneities in the work function of the dosed surface may contribute to the observed change in linewidth.

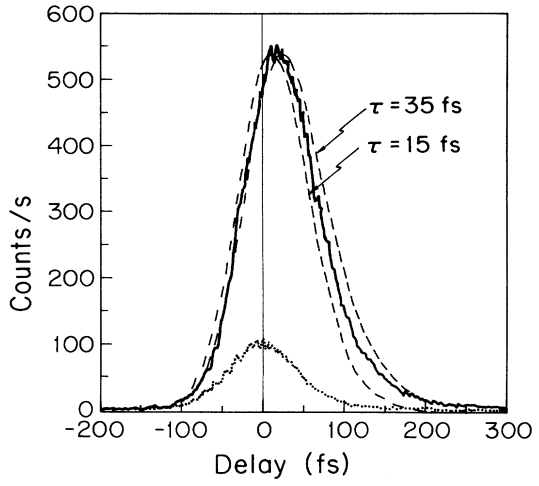

FIG. 3. Lifetime measurements of the $n=1$ image-potential state on a clean Ag(100) surface (solid line) and on an oxygen-dosed surface (dotted line). Dashed lines are convolved exponentials with decay times of 15 and 35 fs.

We can estimate the lifetime of the $n=1$ image-potential state on the clean surface by assuming a simple exponential relaxation. The photoemission response can then be modeled by convolving the uv-visible cross correlation with a single-sided exponential. The dashed lines show such a convolution using the oxygen-dosed data and exponentials of 15 and 35 fs duration. The accuracy of the fits is limited because the relaxation time is less than the pulse duration, and the uv-visible cross correlation is approximate. Nevertheless, from these results we estimate the $n=1$ image-state lifetime to be 25 ± 10 fs.

This lifetime measurement for the lowest-order image state on Ag(100) is consistent with the lower theoretical bound established by early theories of Echenique and Pendry.[24] It is in good agreement with recent predictions for image-state lifetimes on Ag determined using the many-body self-energy formalism.[25] The model predicts relaxation times due to bulk tunneling of several tens of femtoseconds. However, measurements of relaxation dynamics of higher-order image-potential states will provide a more definitive test of theoretical models, and the hydrogenic nature of the wave functions.

The $n=2$ image state on Ag(100) was first identified by Giesen *et al.*[7] using two-photon photoemission. This work determined a binding energy of 0.16 ± 0.02 eV for this state, but as with studies of the $n=1$ state, linewidth broadening measurements did not provide conclusive evidence about the excited-state lifetime. (As of yet, there is no experimental identification of an $n=3$ state on any metal surface.)

In order to populate the $n=2$ state, we require photon energies of at least 4.27 eV. Femtosecond pulses at 4.35 eV are obtained via continuum generation in the pump arm by focusing the amplified 2.0-eV pulses in a 1-mm jet of ethylene glycol formed by a sapphire nozzle. A portion of this continuum in the wavelength range about 570 nm (2.17 eV) is then frequency doubled in a 300-μm crystal of KDP. Frequency discrimination is accomplished using a short-wavelength pass interference filter, in combination with the phase-matching bandwidth of the frequency-doubling crystal. Though the thickness of this crystal introduces some pulse broadening due to phase-matching limitations, the conversion efficiency in thinner crystals was found to be inadequate for this experiment. A pair of quartz prisms is used to compensate second-order dispersion arising from the optical elements, resulting in final pulse durations as short as ~ 80 fs at 285 nm (4.35 eV photon energy).

Figure 1 shows a schematic of the band structure and image-state binding energies on the (100) surface of Ag. Femtosecond pulses at 4.35 eV are used to populate the image states via nonresonant transitions originating below the Fermi level. The high photon energy required to excite the $n=2$ state also generates an electron population in the $n=1$ state with several hundred meV of excess energy. This excess electron energy is in the form of parallel momentum, $k_{\parallel}[100]$, along the crystal surface. Electrons in the $n=2$ state as well as the $n=1$ state are photoemitted to the vacuum by a delayed visible femtosecond pulse at 2.00 eV.

Figure 4 shows photoelectron spectra generated by uv-

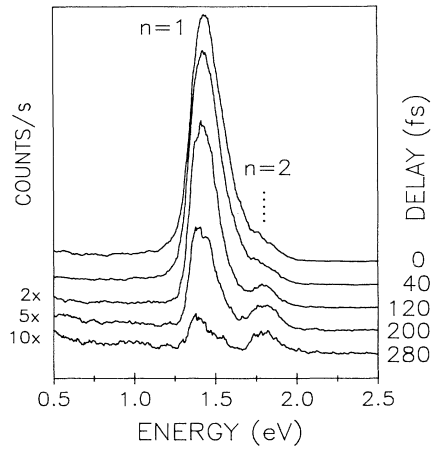

FIG. 4. Photoelectron spectra from Ag(100) using uv-visible two-photon photoemission. Positive delay corresponds to visible pulses arriving after the uv pulses. The peak photoemission signal is ~0.1 electrons/pulse (800 electrons/s).

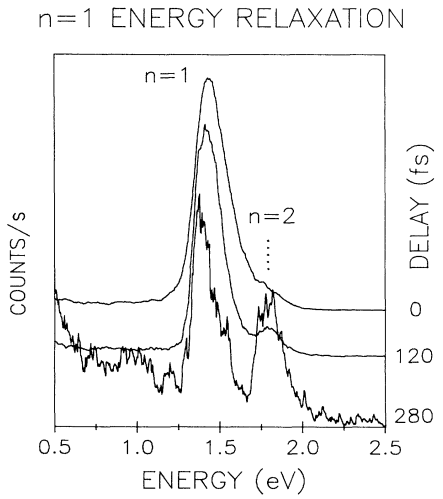

FIG. 5. Normalized (and offset) photoelectron spectra from Ag(100) at various positive delays. Narrowing of the $n=1$ peak with increasing delay is evidence of shorter lifetimes for electrons in states with $k_{\parallel}[100]\neq 0$.

visible two-photon photoemission at various time delays. Visible and uv fluences of ~600 and ~30 $\mu J/cm^2$, respectively, are used to avoid space-charge and nonequilibrium heating effects. Positive delay corresponds to visible probe pulses arriving after the uv pump pulses, and electron energies are measured relative to the vacuum level.

We observe a large peak at ~1.5 eV which corresponds to the $n=1$ image state with a binding energy of ~0.5 eV. Because of the very short lifetime of this state, ~30 fs, the $n=1$ peak disappears very rapidly. However, at longer time delays, a second peak emerges at an energy of ~1.8 eV. This corresponds to the $n=2$ state with a binding energy of ~0.2 eV. With increasing time delay, the height of the $n=2$ peak relative to the $n=1$ peak is observed to increase, suggesting that the $n=2$ state is longer lived.

Though electrons are excited in the $n=1$ band with as much as 400 meV excess energy, the measured energy width of the photoelectron peak corresponding to the $n=1$ state is only ~220 meV. This effect is due to collection angle limitations of the CMA, which makes our measurements most sensitive to electrons near the bottom of the $n=1$ band. However, we are able to observe a slight shift of the $n=1$ peak in the photoelectron spectra of Fig. 4 to lower energies with increasing time, suggesting that electrons with excess parallel momentum are relaxing to $n=1$ image states with lower $k_{\parallel}[100]$, and/or escaping into the crystal by coupling to bulk bands, or surface excitations. This effect is seen more clearly in Fig. 5.

Figure 5 shows photoelectron spectra (normalized to the $n=1$ peak) from Ag(100) at various positive time delays. Near zero delay, the $n=1$ peak is broadest, ~222 meV [full width at half maximum (FWHM)], because electrons are being excited into this state over a range of ~400 meV by the uv pulses (4.35 eV). We do not resolve the entire width of the distribution since electrons in states 400 meV above the bottom of the $n=1$ band will have $k_{\parallel}(100)=0.35$ Å^{-1}. Thus they are emitted from the surface at an angle of ~19° from normal, which is beyond our acceptance angle. After the excitation pulse is gone, at positive delays of 120 and 280 fs, the $n=1$ peak narrows to ~187 and ~142 meV, respectively.

Narrowing occurs due to the relaxation of electrons in higher-energy states. Since the low-energy edge remains fixed, this indicates that higher-energy electrons (electrons with $k_{\parallel}[100]\neq 0$) have shorter lifetimes than electrons at $k_{\parallel}[100]=0$. Shorter lifetimes for electrons with transverse momentum are expected because the number of available states into which these electrons may scatter is increased.[25–27] With increasing transverse momentum the image states begin to overlap with bulk states, the surface band gap shrinks, and bulk scattering effects become stronger. Additionally, high-energy electrons may decay into image states with smaller $k_{\parallel}[100]$.

Quantitative information about the relative lifetimes of the $n=1$ and 2 states is obtained by taking time-resolved scans with the energy analyzer tuned to the peak of each state at 1.5 and 1.8 eV, respectively. These measurements are shown in Fig. 6. The solid lines indicate the transient response of each state, with positive delay corresponding to visible probe pulses arriving after the uv pump pulses. The response of the $n=1$ state is nearly instantaneous, relative to our resolution, although a slight asymmetry toward positive delay is clearly evident. The transient response of the $n=2$ state indicates a lifetime that is substantially longer, on the order of a few hundred femtoseconds. This is consistent with theoretical predictions since higher-order image states have wave functions localized further in the vacuum.[24,27]

An estimate of the $n=2$ image-state lifetime is obtained by assuming a simple exponential relaxation. Under this assumption, we model the transient response by convolving the uv-visible cross correlation with a single-sided exponential. To get an accurate measure of the uv-visible cross correlation at the sample, the sample surface

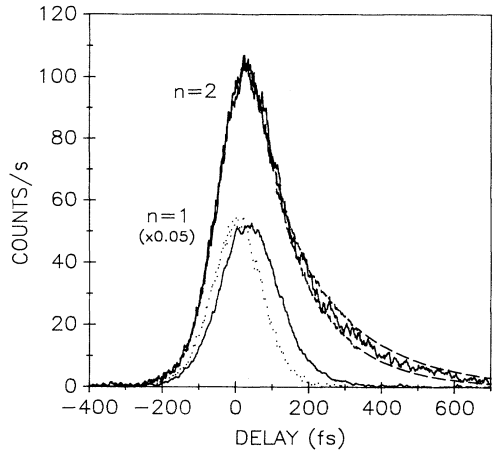

FIG. 6. Transient responses of the $n=1$ and 2 image-potential states on Ag(100) (solid lines). Dashed lines are convolved exponentials with decay times of 160 and 200 fs and $\alpha=0.8$ according to the response model. The dotted line is the normalized uv-visible cross correlation.

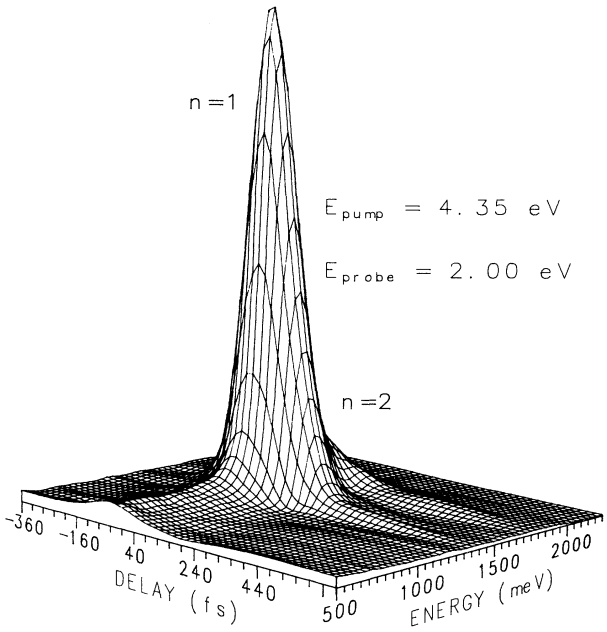

FIG. 7. Relaxation dynamics in time and energy of the $n=1$ and 2 image-potential states on Ag(100). Peak signal ~800 counts/s.

is roughened by ion sputtering. The roughening process effectively quenches the image-state lifetime by providing additional relaxation channels. The result is equivalent to adsorbing oxygen on the surface, but allows us to avoid introducing impurities on the sample. Under these conditions, the transient response of both the $n=1$ and 2 image states is nearly instantaneous, thereby providing a reasonable approximation to the uv-visible cross correlation.

Because of instrument limitations in our angular resolution, the measured response of the $n=2$ state also includes electrons from $n=1$ image states with excess parallel momentum. Thus our model for the $n=2$ transient response also includes some component of the $n=1$ response. This model is described by the following expression:

$$n_2(t)=A(t)\exp(-t/\tau)+\alpha n_1(t)\ ,$$

where $n_2(t)$ is the predicted response, $A(t)$ is the uv-visible cross correlation, τ is the predicted lifetime of the $n=2$ state, and $\alpha n_1(t)$ describes the component of the $n=1$ transient response which contributes to the measurement. Since $k_{\parallel}[100]\neq 0$ electrons in $n=1$ states decay nearly instantaneously, we approximate the $n=1$ response at high energies by the uv-visible cross correlation, $n_1(t)_{k_{\parallel}\neq 0}\approx A(t)$.

The best fits to the $n=2$ response are shown by the dashed lines in Fig. 6. The parameters used in these fits are $\alpha=0.8$ and time constants $\tau=160$ and 200 fs. The measured response falls consistently within these bounds, with the best fit obtained assuming a lifetime of 180 fs. Thus the $n=2$ image-state lifetime, 180±20 fs, on Ag(100) is roughly seven times longer than that reported for the $n=1$ state.

This result demonstrates that image-potential states are well described by a two-dimensional hydrogenic model. The model accounts not only for the n^{-2} dependence of the binding energies, but also predicts wave-function localization in the vacuum resulting in lifetimes which scale as n^3 for higher-order states. Measurements of the $n=1$ and 2 image-state lifetimes on Ag(100) are in good agreement with these predictions. The slight deviation from the n^3 scaling is attributed to the low order of these states, and this issue has been addressed in recent theoretical models.[27]

In addition, since our measurements monitor the occupancy of the $n=1$ and 2 states simultaneously, we should be sensitive to population transfer from the $n=2$ state to the $n=1$ state. This type of relaxation process is not evident in our experimental results. Figure 7 shows the transient dynamics of the $n=1$ and 2 states in time and energy. This manifold is constructed from photoelectron spectra taken at various time delays, and provides an overview of the excited-state dynamics. In order to clarify the surface features, a grid is superimposed over the data using a cubic spline interpolation algorithm. The large peak at ~1.5 eV is the response of the $n=1$ state, which decays quite rapidly. The $n=2$ response is initially obscured by the shoulder of the $n=1$ state, but is more pronounced at later times after the $n=1$ state has decayed. On this longer time scale, we observe an electron population primarily in the $n=2$ state. The correlation signal observed at low energies is attributed to one-photon photoemission enhanced by nonequilibrium electron heating, and two-photon photoemission via virtual states.

B. Image-potential states on Ag(111)

In addition to the measurements of image states on the (100) surface, we have performed studies of the relaxation

dynamics of $n=1$ and 2 image-potential states on the (111) surface of Ag. The characteristics of the (111) surface differ significantly from the properties of the (100) surface. Thus investigations of image-state dynamics on this surface are relevant to understanding the material parameters which affect the lifetime of image-potential states. These measurements represent a more rigorous test of current theoretical models.

In Ag, the relative band gap in the [111] direction is lower in energy than in the (100) direction. As shown in Fig. 8, it extends from 0.31 eV below the Fermi level to 3.85 eV above the Fermi level. The work function for the Ag(111) surface is 4.49 eV, thus the vacuum level lies within the bulk continuum, in marked contrast to the (100) surface where the vacuum level is nearly midgap. As a result, image-potential states on this surface have slightly larger binding energies, and are positioned at higher energies within the bulk band gap.[14,16,24,2] Thus the wave functions for these states are expected to be localized closer to the surface, resulting in shorter lifetimes.[28,26,29]

Two-photon photoemission studies by Giesen *et al.*[5,6] provided the first experimental identification of image-potential states on Ag(111). These studies identified the $n=1$ and 2 states at energies of 3.72 and 4.26 eV above the Fermi level, respectively. The $n=1$ state lies within the gap of projected bulk states, but is near the bulk continuum which exists 3.85 eV above the Fermi level. In contrast, the $n=2$ state lies just outside the band gap, and is therefore resonant with bulk states. In addition, the Ag(111) surface exhibits a crystal-induced surface state which lies 0.12 eV below the Fermi level, and is therefore always occupied. The width of this state is less than 50 meV.[5] Because this "ground" state is localized at the crystal surface, image states may be populated by resonant transitions with greater efficiency than by transitions originating inside the bulk. This can be used to enhance the emission yield from the $n=2$ state which is substantially weaker than that of the $n=1$ state due to wave-function localization in the vacuum.

Relaxation dynamics of the $n=1$ and 2 image-potential states on Ag(111) are performed using the femtosecond ultraviolet pump and visible probe technique described previously. Using continuum generation and frequency doubling combined with dispersion compensation, we are able to generate ~90-fs pulses at 281 nm (4.41 eV).

Figure 8 shows a schematic of the projected band structure at the (111) surface of Ag for $k_{\parallel}[111]=0$ with the $n=1$ and 2 image states at 3.72 and 4.26 eV above the Fermi level, respectively. In the $k_{\parallel}[111]$ direction, the bands are nearly free-electron-like, with $m_{\text{eff}}=1.3m_0$ for the $n=1$ state.[22] Femtosecond pulses at 4.41 eV are used to populate the $n=2$ image-potential state via resonant transitions from the occupied surface state. At the same time, the $n=1$ state is populated via nonresonant transitions originating below the Fermi level. Because of the excess photon energy, the electron distribution in the $n=1$ band will occupy a range of $k_{\parallel}[111]$ states extending several hundred meV from the bottom of the band. As in previous experiments, electrons are photoemitted by delayed visible pulses at 2.00 eV, and both uv and visible pulses are p polarized.

Figure 9 shows the transient dynamics of the $n=1$ and 2 states in time and energy. Ultraviolet and visible fluences are ~25 μJ/cm^2 and ~1.2 mJ/cm^2, respectively. Positive delay corresponds to visible pulses arriving after the uv pulses. We observe two well-defined peaks,

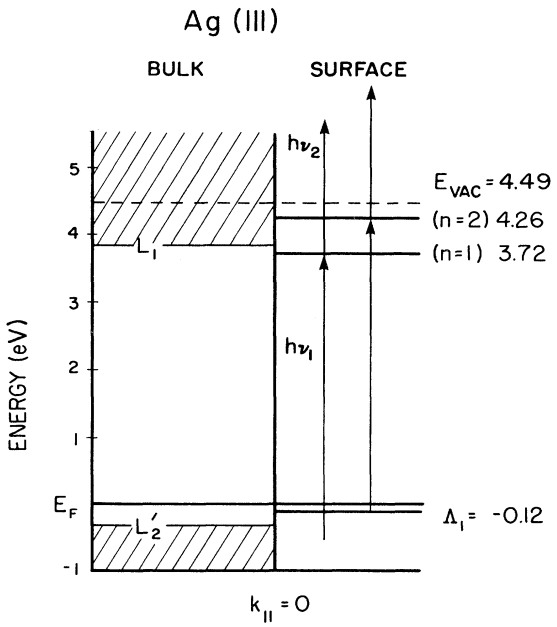

FIG. 8. Energy-level diagram of Ag(111) surface states, and bulk band projections for $k_{\parallel}[100]=0$. Ultraviolet femtosecond pulses, $h\nu_1=4.41$ eV, populate the $n=2$ state via resonant transitions from an occupied surface state, and the $n=1$ state via nonresonant transitions originating below E_F. Visible pulses, $h\nu_2=2.00$ eV, photoemit electrons to the vacuum.

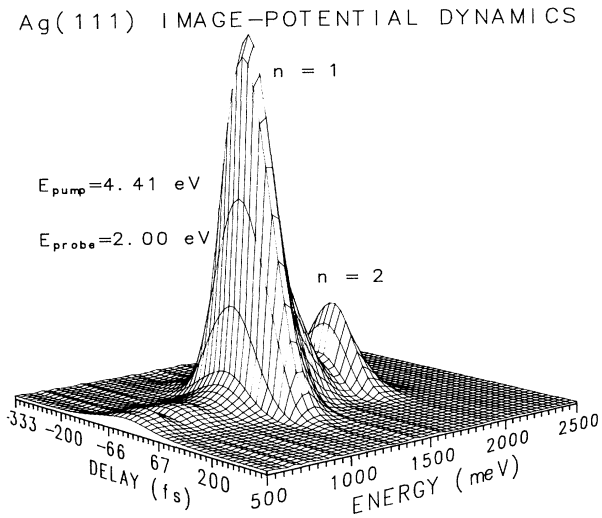

FIG. 9. Transient dynamics of the $n=1$ and 2 image-potential states on Ag(111) in time and energy. Peak photoelectron yield is ~240 counts/s.

one at ~ 1.3 eV and one at ~ 1.8 eV corresponding to photoelectrons from the $n=1$ state (0.77 eV binding energy) and $n=2$ state (0.23 eV binding energy) photoemitted by 2.00-eV femtosecond pulses. In contrast with studies of image-state spectral dynamics on Ag(100) (see Fig. 7), on the (111) surface, the $n=2$ photoelectron peak is well defined even at short time delays. Since the $n=2$ state is resonantly pumped by the 4.41-eV photon energy, the photoelectron yield from this state is enhanced relative to the yield from the $n=1$ state.

Both the $n=1$ and 2 states decay on a time scale comparable to the pulse duration, indicating extremely short lifetimes for both states. Asymmetry toward positive delay, corresponding to a noninstantaneous transient response, does not seem to be evident. Furthermore, the decay of the $n=2$ state appears to be just as rapid as the $n=1$ decay, in marked contrast to the image-state dynamics on Ag(100). This suggests that the placement of the relative gap at $k_{\parallel}[111]=0$ alters the hydrogenic properties of the states. The correlation signal near 500 meV is attributed to two-photon photoemission via virtual states, with a small contribution from nonequilibrium electron heating. The peak photoelectron yield is ~ 240 counts/ (3×10^{-2} electrons/pulse).

More detailed information about the transient dynamics of these states is obtained by taking time-resolved scans at specific energies. Figure 10 shows time-resolved scans obtained with the energy analyzer tuned to the peak of the $n=1$ state and the peak of the $n=2$ state. The height is normalized in order to compare the response widths. The two traces overlap very closely, and neither trace shows any appreciable asymmetry toward positive delay which might indicate a measurable response time. The full width at half maximum is ~ 130 and ~ 115 fs for the $n=1$ and 2 response, respectively.

Differences in lifetime between the $n=1$ state and the $n=2$ state would be manifest as a time shift in the peak of the response, with the longer-lived state being shifted toward positive delay. A wider response width is also expected from the longer-lived state. The transient response of the $n=1$ state is slightly wider, suggesting that this state may be longer lived than the $n=2$ state. This is in agreement with measurements by Giesen *et al.*[5] as well as recent many-body calculations[26] which predict lifetimes of ~ 15 and ~ 11 fs for the $n=1$ and 2 states, respectively. However, because of the presence of the occupied surface state, the 4.41-eV excitation results in an enhanced excited-state electron distribution several hundred meV above the bottom of the $n=1$ band. This distribution may decay to the bottom of the $n=1$ band over a finite period of time, thus contributing to the width of the measured response.

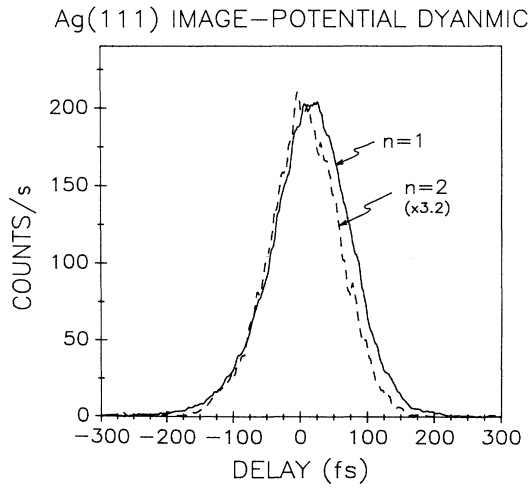

FIG. 10. Transient response of the $n=1$ and 2 image-potential states on Ag(111).

Determination of the temporal resolution of this experiment requires an accurate measure of the uv-visible cross correlation at the sample surface. In our studies of the image-potential dynamics on Ag(100), this cross correlation was approximated by quenching the lifetime of the $n=1$ state by adsorbing oxygen on the sample surface, or by roughening the surface by ion sputtering. In both cases, the reduction of the image-state lifetime was clearly evident by the narrowing of the transient response width, and by the symmetry of the time response in contrast to the asymmetrical time response from a cleaned and annealed surface.

Attempts to quench the lifetimes of the image states on Ag(111) by adsorbing oxygen on the sample surface were not conclusive. The sample was exposed to $\sim 2\times 10^{-2}$ Torr s of oxygen, during which time we monitored the response of the $n=1$ state. No substantial reduction in the photoemission yield was observed, indicating that the oxygen was having no effect on the image state. This was confirmed by subsequent measurements of the photoelectron spectra as well as the $n=1$ transient response, both of which were essentially unchanged compared with preoxygen measurements. This result is not surprising since the Ag(111) surface is known to be virtually unreactive due to the close-packed atomic structure.[30,31]

Similar attempts were made to quench the image-state lifetimes by roughening the sample surface via ion sputtering. This approach was only slightly more successful, possibly because the close-packed surface structure of the (111) plane is less susceptible to atomic disordering than the more open (100) plane. Comparison of photoelectron spectra from a roughened surface with spectra from an annealed surface shows a substantial increase in the energy width of the $n=1$ and 2 states, and a factor of 2 decrease in the peak photoemission yield. This suggests that the relaxation times on the roughened surface may be shorter, although the increased energy width may be attributed to inhomogeneities in the work function of the roughened surface.

The effects of surface roughening on the relaxation dynamics of the image-potential states are shown in Fig. 11. The solid lines represent the transient response of the $n=1$ and 2 image states on an annealed surface. The dashed lines indicate the transient responses of the image states on a roughened surface. In both cases, the data from the roughened surface are normalized to the data from the annealed surface for comparison. For both the $n=1$ state and the $n=2$ state, there is no significant

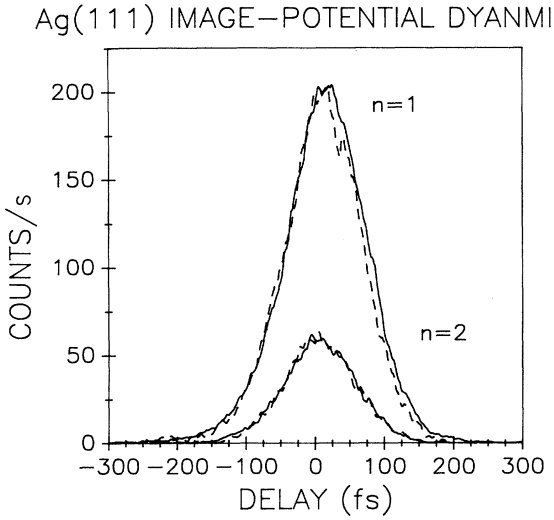

FIG. 11. Transient response of the $n=1$ and 2 image states on Ag(111) from a cleaned and annealed surface (solid lines) and from a roughened surface (dashed lines).

difference in the decay time from the annealed surface versus the sputtered surface. This suggests that any effect of surface roughening on the transient dynamics is not resolved in our measurements. For verification that the surface was disordered during the sputtering process, the LEED pattern was checked. Although a LEED pattern was observed from the surface, the scattered beams were not well defined, indicating that some roughening had occurred.

The decay of the $n=1$ and 2 image-potential states appears to be nearly instantaneous relative to our time resolution, however, the spectral dynamics shown in Fig. 9 suggest that the high-energy electrons in the $n=1$ band decay more rapidly than electrons near the bottom of the band. This effect is evident in Fig. 12 where we measure the photoelectron spectra at delays of 0, +66, and +133 fs. Narrowing of the $n=1$ peak from ~250 meV near zero delay, to ~190 meV at +133 fs delay is clearly evident. Since the low-energy edge of the $n=1$ peak remains fixed, this narrowing is interpreted as evidence that electrons with transverse momentum, $k_{\parallel}[111]\neq 0$, have shorter lifetimes. With increasing transverse momentum, the $n=1$ states will become resonant with the bulk continuum. Additionally, electrons in these states may decay into image states with smaller $k_{\parallel}[111]$. Both of these processes will contribute to the observed effect.

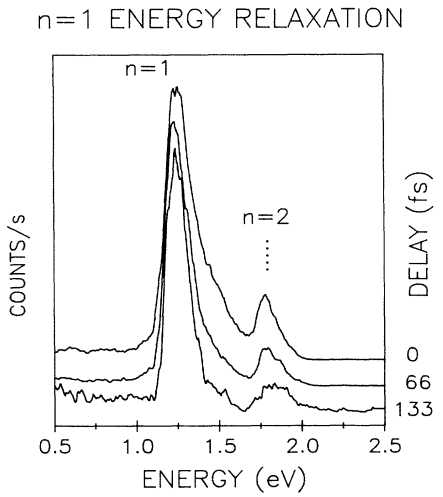

FIG. 12. Normalized (and offset) photoelectron spectra from Ag(111) at various positive delays. Narrowing of the $n=1$ peak with increasing delay is evidence of shorter lifetimes for electrons in states with $k_{\parallel}[111]\neq 0$.

III. DISCUSSION

Studies of the transient dynamics of the $n=1$ and 2 states on the (100) and (111) surfaces of Ag provide information about the behavior of a two-dimensional electron gas in vacuum. The measured lifetimes from the (100) surface are substantially longer than predicted bulk relaxation times, suggesting that these states are decoupled from the lattice due to wave-function localization in the vacuum. Measurements taken on the (111) surface show somewhat shorter lifetimes, suggesting that image-potential states on this surface are more strongly coupled to bulk processes. These measurements are an important test of theoretical models since the image-state lifetimes and lifetime scaling with n indicate the relative influence of the bulk and the $1/R$ Coulomb potential on the image-potential states.

Echenique and Pendry[24] developed the first comprehensive theory of image-potential states, based on a phase-shift multiple-scattering model. A Rydberg-like series of bound states is established by resonances in the wave function, due to scattering from the image-potential barrier and from the crystal surface. The lifetime broadening of these states is governed primarily by the wave-function overlap with the bulk, because this overlap determines the extent to which the image state is affected by bulk relaxation processes. By matching hydrogenic wave functions at the crystal surface to wave functions decaying into the bulk, the wave-function overlap with this region of finite absorption can be shown to scale as n^{-3}. Thus higher-order states should exhibit diminished energy broadening corresponding to longer lifetimes scaling as n^3.

Echenique and Pendry calculate image-state lifetimes by modeling the decay process with an imaginary component of the wave-function self-energy.[24] Since the self-energy is overestimated in these calculations, the predicted lifetimes: $\tau_{n=1}=2$ fs, $\tau_{n=2}=13$ fs, and $\tau_{n=3}=44$ fs, represent lower bounds for these states. However, the predicted lifetime scaling, $\tau_n \sim n^3$ for $n>2$, and $\tau_{n=2}/\tau_{n=1}\approx 6$, comes from the assumed $1/R$ dependence of the image potential.[24] Our experimental measurements from the Ag(100) surface are in good agreement with this lifetime scaling and suggest that image-potential states on Ag(100) are well described by hydrogenic wave functions with properties determined largely by the Coulombic surface potential barrier.

Lifetime measurements of image states on Ag(100) are also consistent with recent theoretical calculations by de Andrés *et al.*[27] in which the lifetime broadenings of the image states are calculated as a function of the state quantum number n. The calculation corresponds with the properties of Ag(100), since a hydrogenic model with an infinite barrier is assumed. The lifetime broadening exhibits an n^{-3} dependence for states with $n \geq 5$. For states $n < 5$, the linewidth broadening is between n^{-3} and n^{-2}, with $\Delta E_{n=1} \approx 4\Delta E_{n=2}$. Because the model neglects the wave-function penetration in the bulk for the lower states, the lifetime broadening of these states is underestimated.

Recently, specific relaxation mechanisms and associated lifetimes of $n=1$ image-potential states have been modeled theoretically by a number of workers using many-body calculations of the wave-function self-energy.[29,25–27] Echenique *et al.*[25] have used this approach to calculate image-state lifetime broadening resulting from two relaxation mechanisms: decay from the bottom of the image-state band into empty bulk states via electron-hole excitation (tunneling through the crystal barrier), and decay into image-potential states having smaller parallel momentum (intraband relaxation). For the $n=1$ state on Ag(100), Echenique *et al.*[25] predict linewidth broadening (ΔE_{FWHM}) due to bulk tunneling on the order of 3 meV (220 fs) to 28 meV (24 fs), and interband relaxation on a comparable time scale. Experimental measurements of the image-state dynamics on Ag(100) ($15 < \tau_{n=1} < 35$ fs) are in reasonable agreement with this theoretical prediction. Discrepancies between theory and experiment may be attributed to chosen parameters of the image-state wave functions, or to uncertainties in the surface response function. In addition, decay mechanisms which the theory does not consider (such as bulk tunneling from image states at $k_{\parallel} \neq 0$) may contribute to the measured lifetimes.

On the (111) surface of Ag, consideration of wave-function overlap is particularly important since the proximity of the edge of the gap allows image-potential states to extend a significant distance into the crystal.[28,29] This accounts for the rapid dynamics observed on Ag(111), where we measure an $n=1$ excited-state lifetime <20 fs. In contrast, image-potential states on the (100) surface are bound by a large crystal potential barrier because the vacuum level is nearly midgap relative to the bulk band continuum.

Image-state lifetimes for the (111) surfaces of Ag have been calculated by de Andrés *et al.*[26] using the same self-energy formalism. For the $n=1$ state, inelastic relaxation processes (e.g., electron-hole excitation in the bulk) are found to dominate. The calculated energy broadening displays a nearly linear dependence on the assumed wave-function penetration, varying from $\Delta E_{\mathrm{FWHM}} = 22$ meV (30 fs), assuming 10% penetration to $\Delta E_{\mathrm{FWHM}} = 184$ meV (3.6 fs), assuming 99% penetration.

Furthermore, calculations for lifetime broadening of the $n=2$ state exhibit a substantial contribution from elastic (electron-electron) scattering effects. This is due to the fact that the $n=2$ state is resonant with the bulk band continuum. Thus elastic scattering can take electrons from the $n=2$ state to bulk states at different points of the Brillouin zone. de Andrés *et al.*[26] calculate energy widths (FWHM) of 44 meV (15 fs) and 58 meV (11 fs) for the $n=1$ and 2 states, respectively, on Ag(111). Measurements of image-state lifetimes of Ag(111) are consistent with these theoretical predictions. Not only are relaxation times substantially faster than those observed from the (100) surface, but measurements suggest that the $n=2$ state on Ag(111) is shorter lived than the $n=1$ state.

Finally, the experimental measurements of the $n=1$ state on both the (100) and (111) surfaces suggest shorter lifetimes for image-potential states with $k_{\parallel} \neq 0$. This may be due to enhancement of the bulk tunneling process and/or relaxation to image states with smaller $k_{\parallel}$ on roughly the same time scale.[25–27]

IV. SUMMARY

In summary, the transient dynamics of image-potential states on Ag(100) and Ag(111) have been investigated using time-resolved two-photon photoemission with femtosecond pulses in the visible at 2.00 eV, and in the uv region from 4.00 to 4.35 eV. This two-color technique, with uv pulses populating the image states, and visible pulses photoemitting from the image states to the vacuum, permits nearly background-free measurements of the image-state dynamics in both time and energy.

Measurements on the (100) surface of Ag demonstrate an excited-state lifetime $\tau = 25 \pm 10$ fs for the $n=1$ state, and $\tau = 180 \pm 20$ fs for the $n=2$ state. These lifetimes are much longer than excited-state lifetimes in the bulk, suggesting that these states are decoupled from the lattice due to wave-function localization in the vacuum. The scaling of the lifetime with n ($\tau_n \sim n^3$) is indicative of the hydrogenic nature of the image-potential states on this surface, and is predicted by theory.[24,27] In addition, the $n=1$ lifetime compares reasonably well with recent theoretical models[25] which estimate lifetime broadening ($\Delta E_{n=1} \sim 10$ meV) due to decay into empty bulk states from image states at $k_{\parallel}[100] = 0$. This corresponds to image-state lifetimes on the order of 70 fs.

The transient dynamics of the $n=1$ and 2 image-potential states on Ag(111) have been investigated in order to determine the effect of the bulk band-gap position on the properties of the states. Our measurements indicate lifetimes of less than 20 fs for both the $n=1$ and 2 image states, substantially shorter than image-state lifetimes on the (100) surface of Ag. These results suggest that image-potential states which lie near the edge of the bulk band gap experience a smaller potential barrier at the surface. Hence image-state wave functions will penetrate further in the bulk, resulting in shorter lifetimes. In addition, the $n=2$ state decays rapidly because it lies outside the bulk band gap, and is therefore resonant with short-lived free-electron states in the solid. The observed behavior is consistent with theoretical predictions for $n=1$ and 2 states on Ag(111).[26]

Spectral measurements also indicate energy relaxation dynamics within the $n=1$ band on both Ag(100) and Ag(111) surfaces. The measurements are evidence that

electrons with excess parallel momentum, $k_{\parallel}$, have shorter lifetimes. These high-energy electrons are able to tunnel into the bulk more easily, and can also decay to image states with lower parallel momentum. Our results do not indicate substantial population transfer from the $n=2$ to the $n=1$ state.

Further studies using angle-resolved photoemission techniques should enable the dynamics of the two-dimensional electron gas in the image-potential state to be characterized in terms of the excess parallel momentum of the electrons. Additionally, by adsorbing impurities on the sample surface, the position of the image states within the bulk band gap may be controlled. In the case of the Ag(111) surface, impurities may be used to move the image states toward the middle of the band gap, perhaps lengthening the lifetime of the states.

ACKNOWLEDGMENTS

This research was supported in part by the Air Force Office of Scientific Research under Contract No. F49620-880C-0089, the Joint Services Electronics Program under Contract No. DAAL03-89-C-0001, the AT&T Foundation, and a grant from IBM. R.W.S. gratefully acknowledges support from Newport Corporation. J.G.F. gratefully acknowledges support from National Science Foundation Grant No. ECS-8552701.

*Present address: Lawrence Berkeley Laboratory, Berkeley, CA 94720.

[1]W. Shockley, Phys. Rev. **56**, 317 (1939).
[2]M. W. Cole and M. H. Cohen, Phys. Rev. Lett. **23**, 1238 (1969).
[3]P. D. Johnson and N. V. Smith, Phys. Rev. Lett. **49**, 290 (1982).
[4]P. D. Johnson and N. V. Smith, Phys. Rev. B **27**, 2527 (1983).
[5]K. Giesen, F. Hage, F. J. Himpsel, H. J. Riess, and W. Steinmann, Phys. Rev. Lett. **55**, 300 (1985).
[6]K. Giesen, F. Hage, F. J. Himpsel, H. J. Riess, and W. Steinmann, Phys. Rev. B **33**, 5241 (1986).
[7]K. Giesen, F. Hage, F. J. Himpsel, H. J. Riess, and W. Steinmann, Phys. Rev. B **35**, 971 (1987).
[8]W. Steinmann, Appl. Phys. A **49**, 365 (1989).
[9]B. Reihl, R. R. Schlittler, and H. Neff, Phys. Rev. Lett. **52**, 1826 (1984).
[10]B. Reihl, K. H. Frank, and R. R. Schlittler, Phys. Rev. B **30**, 7328 (1984).
[11]N. Garcia, B. Reihl, K. H. Frank, and A. R. Williams, Phys. Rev. Lett. **54**, 591 (1985).
[12]A. Goldmann, V. Dose, and G. Borstel, Phys. Rev. B **32**, 1971 (1985).
[13]S. L. Hulbert, P. D. Johnson, N. G. Stoffel, and N. V. Smith, Phys. Rev. B **32**, 3451 (1985).
[14]D. Straub and F. J. Himpsel, Phys. Rev. B **33**, 2256 (1986).
[15]D. Straub and F. J. Himpsel, Phys. Rev. Lett. **52**, 1922 (1984).
[16]S. L. Hulbert, P. D. Johnson, N. G. Stoffel, W. A. Royer, and N. V. Smith, Phys. Rev. B **31**, 6815 (1985).
[17]R. W. Schoenlein, J. G. Fujimoto, G. L. Eesley, and T. W. Capehart, Phys. Rev. Lett. **61**, 2596 (1988).
[18]R. W. Schoenlein, J. G. Fujimoto, G. L. Eesley, and T. W. Capehart, Phys. Rev. B **41**, 5436 (1990).
[19]J. Valdmanis, R. Fork, and J. Gordon, Opt. Lett. **10**, 131 (1985).
[20]W. Knox, M. Downer, R. Fork, and C. Shank, Opt. Lett. **9**, 552 (1984).
[21]R. Fork, O. Martinez, and J. Gordon, Opt. Lett. **9**, 150 (1984).
[22]K. Giesen, F. Hage, F. J. Himpsel, H. J. Riess, and W. Steinmann, Phys. Rev. B **35**, 975 (1987).
[23]R. Schoenlein, W. Lin, J. Fujimoto, and G. Eesley, Phys. Rev. Lett. **58**, 1680 (1987).
[24]P. M. Echenique and J. B. Pendry, J. Phys. C. **11**, 2065 (1978).
[25]P. M. Echenique, F. Flores, and F. Sols, Phys. Rev. Lett. **55**, 2348 (1985).
[26]P. de Andrés, P. M. Echenique, and F. Flores, Phys. Rev. B **35**, 4529 (1987).
[27]P. de Andrés, P. M. Echenique, and F. Flores, Phys. Rev. B **39**, 10 356 (1989).
[28]M. Weinert, S. L. Hulbert, and P. D. Johnson, Phys. Rev. Lett. **55**, 2055 (1985).
[29]J. Bausells, P. M. Echenique, and F. Flores, Surf. Sci. **178**, 268 (1986).
[30]R. W. Joyner and M. Roberts, Chem. Phys. Lett. **60**, 459 (1979).
[31]G. Rovida, F. Pratesi, M. Maglietta, and E. Ferroni, Surf. Sci. **43**, 230 (1974).